Size-dependent Resistivity of Metal Electrodes in $BiFeO_3$ Crossbar Structures

Budi Mulyanto

***Abstract*—In this work, the size-dependent resistivity effect in some metals used as the crossbar electrodes were discussed. The ideal crossbar structure should have a footprint of $4F^2$ with F is the allowed minimum structure width at the technology at which the crossbar is implemented. This motivates us to take a look into a size-dependent resistivity effects. This effects are relevant not only in this structures but also in the microelectronics fabrication in general. The increase in the resistivity which is caused by the electron scattering at the wire surface and at grain boundaries are modeled in Fuchs-Sondheimer and Mayadas-Shatzkes model, respectively. The calculation of the increased resistivity allows us to simulate the crossbar circuit closer to reality.**

***Index Terms*—Nanowire Resistance, Resistive Switching, Memristor, $BiFeO_3$ (BFO), Crossbar.**

I. Introduction

In order to design the ASIC, either in Moore regime, Beyond Moore, or More than Moore, the designers require information regarding the technology node they are using. This information is compiled by the manufacturers and given to the designers as Process Design Kits (PDKs) which contain device models and parameters and other physical information. One of the information is the sheet resistances of the metal layers which will be used during the design process, e.g. during the parasitic extraction. This motivates the research in the field of electrical characterization of thin films and nanowires.

One of the advantages of the crossbar structures is its small footprint. The ideal crossbar structure should have a footprint of $4F^2$ with F is the allowed minimum structure width at the technology at which the crossbar is implemented. Figure 1 shows the picture of bottom electrode of a 10 x 10 crossbar structure that was fabricated in this work. The width of the track is $20\,\mu\mathrm{m}$.

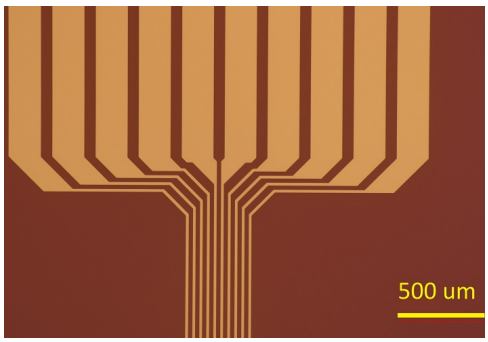

Fig. 1. The fabricated 10 x 10 Crossbar' bottom electrode.

It has been well known since 1930s, that the resistivity of thin films depends on the size. On the films with a few atomic layer thickness, the resistivity deviates larger then the bulk [1] [2]. Those two papers argued that the deviation is because electron scattering when it reaches the film surface. Later Chamber [3] developed a model to predict the size-dependent resistivity of small wires with arbitrary cross section. His model will be used here. The basis of this model is the conservation of electron momentum after it collides with the surface. This scattering mechanism is described by one parameter, specularity p. If the electrons keeps theirs momentum along the direction of the electrical field, it is categorized as specular (p = 1). Changing of momentum causes the reduction of of the total net current. So, in the case of $p < 1$, purely or partially diffused, the resistivity is higher [4]. Figure 2 helps giving a graphical information about this mechanism.

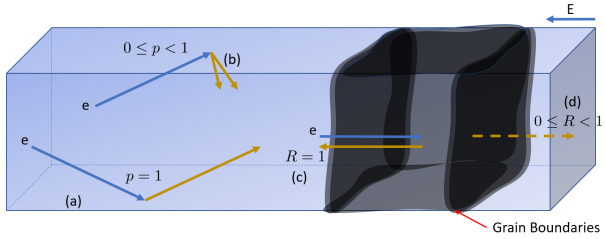

Fig. 2. The picture provides a description of the surface scattering mechanism. Only the momentum along the electric field direction is considered. On the specular case (a), the momentum along the electrical field direction is conserved. While on the diffuse scattering, it is not. (b) If $0 \leq p < 1$, it considered as partly diffused while the completely diffused scattering has p = 0. Grain boundary scattering is described in (c) and (d), for R = 1 and $0 \leq R < 1$, respectively.

The rest of this report is structured as follows. In Section II, the basic theories about the size-dependent resistivity is explained. Two electron scattering mechanism are explained in this section and are related to define the size-dependent resistivity in thin wires with rectangular cross section. Section III gives the simulation result of the size-dependent resistivity based on Fuchs-Sondheimer model (FS model) and Mayadas-Shatzkes model (MS model). Section IV shows resistance calculation of the top pad structure using Finite Difference Method (FDM). The work is ended by a summary.

II. Size-dependent Resistivity

A. Fuchs-Sondheimer model (FS model)

Chamber provided us the formula for the resistivity for arbitrary cross sectional geometry. The paper covers both specular and diffused surface scattering. s refers to the cross-sectional area, ϕ is the azimuth angle, and θ is the altitude angle. ρ_{FS} represent the (scaled) resistivity due to surface

TABLE I
EQUATIONS FOR ELECTRON TRAVELING PATH INSIDE THE WIRES AND THEIR ASSOCIATED ANGLES. NOTE: ϕ_4 AND ϕ_5 REPRESENT THE SAME ANGLE.

$\lvert OP\rvert$	Related Angles	List of angle definitions
$\lvert OP\rvert_{\text{CD}} = \frac{h-y}{\sin\theta\sin\phi}$	ϕ_1, ϕ_2	$\phi_1 = \arctan\left(\frac{h-y}{w-x}\right)$
$\lvert OP\rvert_{\text{DA}} = \frac{-x}{\sin\theta\cos\phi}$	ϕ_2, ϕ_3	$\phi_2 = \arctan\left(\frac{x}{h-y}\right) + \frac{\pi}{2}$
$\lvert OP\rvert_{\text{AB}} = \frac{-y}{\sin\theta\sin\phi}$	ϕ_3, ϕ_4	$\phi_3 = \arctan\left(\frac{y}{x}\right) + \pi$
$\lvert OP\rvert_{\text{BC}} = \frac{w-x}{\sin\theta\cos\phi}$	ϕ_5, ϕ_1	$\phi_4 = \arctan\left(\frac{w-x}{y}\right) + \frac{3\pi}{2}$
		$\phi_5 = -\arctan\left(\frac{y}{w-x}\right)$

scattering and is associated with Fuchs-Sondheimer model (FS model). OP is the length of electron traveling path inside the small wires and λ is the electron free mean path. The definition of OP is dependent of geometry and mathematical choice of coordinate reference.

$$\frac{\rho_{\text{bulk}}}{\rho_{\text{FS}}} = \frac{3}{4\pi \text{s}} \int_s ds \int_0^{2\pi} d\phi \int_0^{\pi} d\theta \sin\theta \cos^2\theta \left(1 - e^{-(\frac{OP}{\lambda})}\right) \tag{1}$$

The detail guidance how to define the electron traveling path and the integration can be found in [5]. The same paper also provides some calculation result for small wires of Ag to compare to our own simulation. A small but important note about the calculation is, depending on the electron traveling path definitions, the integration can be a nested one, i.e. it might become a quadruple integration without variable separation possibility. For the pure diffused scattering, the equation is:

$$\frac{\rho_{\text{bulk}}}{\rho_{\text{FS}}}(p=0,\lambda) = \frac{3}{4\pi \text{hw}} \int_0^{w} dx \int_0^{h} dy \sum \int_{\phi_{\text{i}}}^{\phi_{\text{j}}} d\phi \quad ... \\ \int_0^{\pi/2} d\theta \sin\theta \cos^2\theta (1 - e^{-(\frac{|OP|_{\text{XX}}}{\lambda})}) \tag{2}$$

As it has been mentioned above, a thin wire with rectangular cross section will be assumed and this cross sectional geometry influences how the electron traveling path is defined mathematically. The diagram for this thin wire can be seen in Figure 3a with electron traveling path OP generally described. Figure 3b depicts the definitions of the all possible azimuthal angles for rectangular cross sectional wires. Both pictures can help us to write the equations for OP that later are substituted into Equation (2). The notation XX in $|OP|_{\text{XX}}$ refers to the sides of the rectangular cross section, e.g., with the help of figure 3b, XX can be CD, DA, AB, and BC. Point $O(x,y,z)$ is the origin point of the electron and it can be anywhere within the wires. Point $P(x',y',z')$ is the collision point of electron with the surfaces. The projection of $P(x',y',z')$ onto the cross sectional area is point $K(x',y',z)$ and $\angle OKP = 90°$. Point $K(x',y',z)$ can be anywhere at the circumference of rectangular ABCD. ϕ_{i} and ϕ_{j} depend on $|OP|_{\text{XX}}$ and the detail for them can be seen in Table I.

B. Mayadas-Shatzkes model (MS model)

In addition to the surface scattering, the electrons also experience scattering in the grain boundaries [6]. The model in

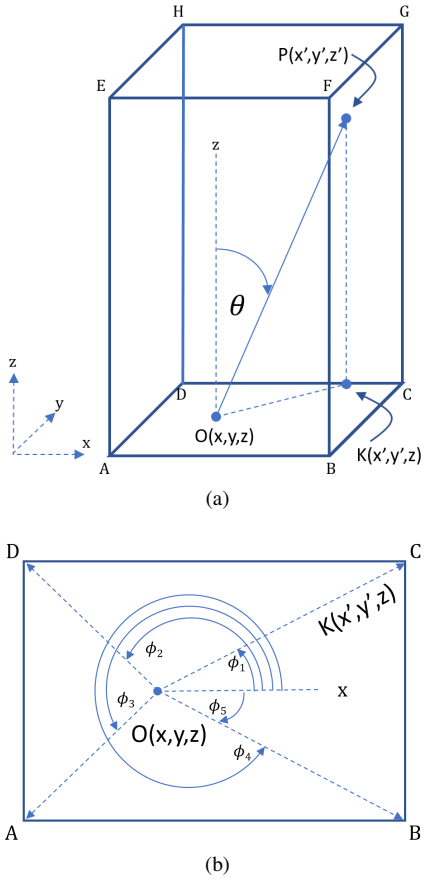

Fig. 3. (a) This is the diagram of a thin wire with rectangular cross section. The diagram can help us in defining the equation for electron traveling path inside the wire. (b) Cross sectional diagram of wire in (a) with all possible azimuthal angle definitions, assuming different collision point on the surface.

[6] described the back scattering, surface scattering, and grain boundaries scattering for polycrystalline metal films. Later, this is referred as Mayadas-Shatzkes model (MS model).

The original MS model is focus on thin films, i.e., the planar dimension is much larger than the thickness. What [4] did was to adapt the original MS model so it is suitable for thin wires, i.e., one planar dimension is much more smaller than the other one by including the size-dependent average grain size which discussed in [7]. Reference [7] defines the width dependent average grain size by dividing the total length of all possible average grain length larger than the width of the wires by the probable number of such grains.

The formulas from [4] (3) and some model interpretation formed in (4) from [7] will be used. As explained before, the modified MS model now considers the size-dependent average grain size. Equation 3 is from [7] and it describes the average grain size on the wire. The grain size follow lognormal distribution which is written as $f(D)$ in this equation. D_{eff} is the average grain length in the thin wires and depends on the width of the wires. D_{50} is the median of diameter of the grain in original scale (not the log value). σ is the standard deviation of $log(D)$ or the standard deviation in the log value. Equation (4) is now as a function of wire width. λ is the electron mean free path. R is the electron reflection ratio at the grain boundary. ρ_{MS} represent the (scaled) resistivity due

to grain boundary scattering and is associated with FS model.

$$D_{eff} = \frac{\frac{\pi}{4}\int_w^\infty f(D) D \frac{D-w}{w} \mathrm{d}D}{\int_w^\infty f(D)\frac{D-w}{w}\mathrm{d}D}, \quad \text{with} \quad f(D) = \frac{1}{\sigma D\sqrt{2\pi}} \exp\left\{-\left[\frac{1}{\sigma\sqrt{2}} ln\left(\frac{D}{D_{50}}\right)\right]^2\right\} \tag{3}$$

$$\frac{\rho_{\text{bulk}}}{\rho_{\text{MS}}} = 3\left[\frac{1}{3} - \frac{\alpha}{2} + \alpha^2 - \alpha^3 ln\left(1+\frac{1}{\alpha}\right)\right], \quad \text{with} \quad \alpha = \frac{\lambda}{D_{eff}}\frac{R}{1-R} \tag{4}$$

If ρ_{FS} and ρ_{MS} have already calculated, the total resistivity is considered as the bulk resistivity added with the resistivity increments which come from surface scattering and grain boundary scattering. [5]

$$\rho = \rho_{\text{bulk}} + (\rho_{\text{FS}} - \rho_{\text{bulk}}) + (\rho_{\text{MS}} - \rho_{\text{bulk}}) \tag{5}$$

Both models are semi classical model. It fits experimental data well but it is important to note that it does not include confinement effect and other quantum mechanical related effects [8]. This is also the reason that the models does not give suggestion how to improve the conductivity [9] while more advance model can give some insight and suggestions [8].

III. Tracks Resistance Calculation

The resistivity for the top and bottom electrodes of the crossbar structure were calculated. A simple Octave script is used to simulate the size-dependent resistivity effect. Table II summarizes all the parameters needed. The same table also contains the size-dependent resistivity as the calculation result. It can be seen that the resistivity values do not vary to much from the bulk in these dimensions. Nevertheless, the motivation of investigating this size-dependent resistivity is to accommodate the design change, same like the one of writing the macros to generate the layout. Finally, the total resistivity is the total increment of FS and MS contribution to the bulk resistivity as can be seen in Equation (5).

Following this formula, the total resistivity of the Gold top track is $2.4318\,\mu\Omega cm$. For the bottom electrode, the total resistivity for Pt and Ti are $11.254\,\mu\Omega cm$ and $99.319\,\mu\Omega cm$, respectively. All of the results are higher than the bulk but does not deviate as much as the wires with smaller size like discussed in the paper [4].

From the calculated resistivity values, the following line and track resistance have been calculated by the software LayoutEditor. For the bottom electrode, the resistance of Pt layer and Ti layer are calculated separately and the parallel resistance is calculated after that. An example of the calculation result for crossbar 3 x 3 is shown in Figure 4.

TABLE II
FS and MS model result for the top and bottom electrodes. The width is uniform, 20 µm. * assumed, ** assumed and for fitting

Model	Quantity	Unit	Au	Pt	Ti
FS	ρ_0	$[\mu\Omega cm]$	2.20 [11]	10.5 [12]	75 [14]
	λ	$[nm]$	40 [4]	23 [13]	18 [15]
	p	$[--]$	0 *, 0.5 [4]	0 *, 1 [13]	0 *, 1 [15]
	h	$[nm]$	180	150	30
	ρ_{FS}	$[\mu\Omega cm]$	2.4159	11.225	99.293
MS	σ	$[--]$	0.2 [4]	0.385 [17]	0.246 [16]
	D_{50}	$[nm]$	40 [4]	23.212 [17]	31.045 [16]
	R	$[--]$	0.9 [4], 0.658**	0.57 [13]	0.17 [15]
	$grainsize$	$[nm]$	40.808±8.244 [4]	25±10 [17]	32±8 [16]
	ρ_{MS}	$[\mu\Omega cm]$	2.2159	10.529	75.026
Total	ρ	$[\mu\Omega cm]$	2.4318	11.254	99.319

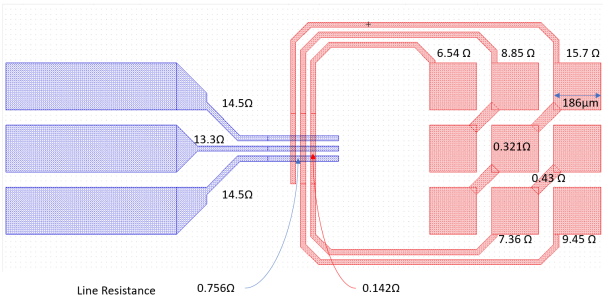

Fig. 4. Bottom electrode resistance for crossbar 3 x 3.

IV. Top Pad Resistance Calculation

For characterization purpose, the resistance of the diamond-shaped top pad resistance was needed. The software LayoutEditor can actually calculate this using its own numerical method. However, it would be good if a comparison was made and this calculation is for that purpose. Gauss-Seidel (and Relaxation) algorithm is used due it its simplicity.

Due to symmetry, the top pad can be divided into four equal shapes. This calculation only calculates this quarter.The final resistance can be found by multiply the result by four. Figure 5 shows this a quarter of the top pad.

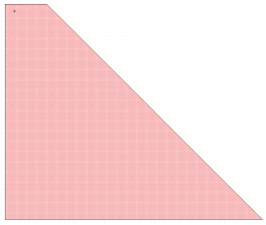

Fig. 5. A quarter of top pad structure.

The equation that need to be solved is shown in 6. This equation can be solved numerically and for this purpose, Gauss-Seidel (and Relaxation) algorithm is used due it its simplicity. This algorithm is written in Equation (7). A short Octave script was written to perform this algorithm.

$$\begin{aligned} \nabla \cdot J &= \frac{\partial \rho}{\partial t} = 0 \\ \nabla \cdot \sigma E &= \nabla \cdot \sigma(-\nabla V) = -\sigma \nabla^2 V = 0 \\ \nabla^2 V &= 0 \end{aligned} \tag{6}$$

$$f_{i,j}^{n+1} = f_{i,j}^{n} + R\left(\frac{f_{i+1,j}^{n} + f_{i-1,j}^{n+1} + f_{i,j+1}^{n} + f_{i,j-1}^{n+1}}{4} - f_{i,j}^{n}\right) \tag{7}$$

The result are shown in Figure 6. The top pad resistance obtained through this calculation and the result from the LayoutEditor at the finest accuracy were $0.295\,31\,\Omega$ and $0.299\,\Omega$, respectively.

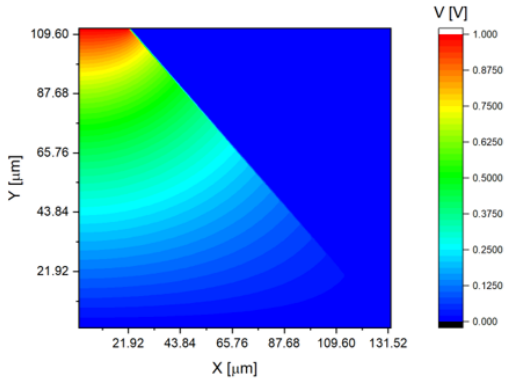

(a)

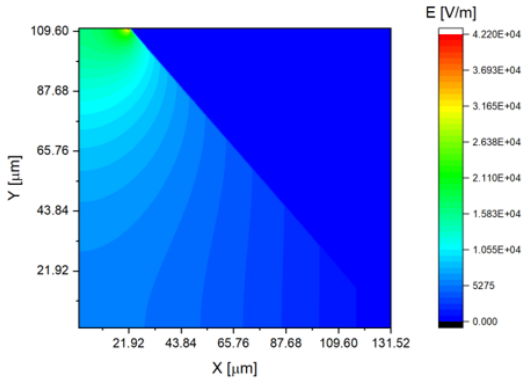

(b)

Fig. 6. (a) The potential, V (b) The electric field, E

V. Summary

The resistance of the tracks have been also calculated. Due to the size-dependent effect, resistivity of the Gold top electrode and Pt bottom electrode has been estimated using Fuchs-Sondheimer and Mayadas-Shatzkes Model for surface scattering and grain boundaries scattering contribution to the resistivity, respectively. The simulation results the resistivity is $2.4318\,\mu\Omega$cm, $11.254\,\mu\Omega$cm, $99.319\,\mu\Omega$cm for Au, Pt, and Ti, respectively. Both models do not cover confinement and other quantum mechanical effects. Mode advance models are required to include these effect to the resistivity estimation. The resistivity values are then used to calculate the track resistance and this can be done with the help of LayoutEditor.

References

[1] K. Fuchs and N. F. Mott, "The conductivity of thin metallic films according to the electron theory of metals," *Mathematical Proceedings of the Cambridge Philosophical Society*, vol. 34, no. 01, p. 100, jan 1938. [Online]. Available: https://doi.org/10.1017/s0305004100019952

[2] E. Sondheimer, "The mean free path of electrons in metals," *Advances in Physics*, vol. 1, no. 1, pp. 1–42, jan 1952. [Online]. Available: https://doi.org/10.1080/00018735200101151

[3] R. G. Chambers and W. L. Bragg, "The conductivity of thin wires in a magnetic field," *Proceedings of the Royal Society of London. Series A. Mathematical and Physical Sciences*, vol. 202, no. 1070, pp. 378–394, aug 1950. [Online]. Available: https://doi.org/10.1098/rspa.1950.0107

[4] C. Durkan and M. E. Welland, "Size effects in the electrical resistivity of polycrystalline nanowires," *Physical Review B*, vol. 61, no. 20, pp. 14 215–14 218, may 2000. [Online]. Available: https://doi.org/10.1103/physrevb.61.14215

[5] D. Josell, C. Burkhard, Y. Li, Y.-W. Cheng, R. R. Keller, C. A. Witt, D. R. Kelley, J. E. Bonevich, B. C. Baker, and T. P. Moffat, "Electrical properties of superfilled sub-micrometer silver metallizations," *Journal of Applied Physics*, vol. 96, no. 1, pp. 759–768, jul 2004. [Online]. Available: https://doi.org/10.1063/1.1757655

[6] A. F. Mayadas and M. Shatzkes, "Electrical-resistivity model for polycrystalline films: the case of arbitrary reflection at external surfaces," *Physical Review B*, vol. 1, no. 4, pp. 1382–1389, feb 1970. [Online]. Available: https://doi.org/10.1103/physrevb.1.1382

[7] Y.-C. Joo and C. V. Thompson, "Analytic model for the grain structures of near-bamboo interconnects," *Journal of Applied Physics*, vol. 76, no. 11, pp. 7339–7346, dec 1994. [Online]. Available: https://doi.org/10.1063/1.357979

[8] K. Moors, B. Soree, and W. Magnus, "Modeling and tackling resistivity scaling in metal nanowires," in *2015 International Conference on Simulation of Semiconductor Processes and Devices (SISPAD)*. IEEE, sep 2015. [Online]. Available: https://doi.org/10.1109/sispad.2015.7292299

[9] B. Feldman, R. Deng, and S. T. Dunham, "Dependence of resistivity on surface profile in nanoscale metal films and wires," *Journal of Applied Physics*, vol. 103, no. 11, p. 113715, jun 2008. [Online]. Available: https://doi.org/10.1063/1.2937085

[10] U. Schmid and H. Seidel, "Effect of high temperature annealing on the electrical performance of titanium/platinum thin films," *Thin Solid Films*, vol. 516, no. 6, pp. 898–906, jan 2008. [Online]. Available: https://doi.org/10.1016/j.tsf.2007.04.128

[11] A. Bietsch and B. Michel, "Size and grain-boundary effects of a gold nanowire measured by conducting atomic force microscopy," *Applied Physics Letters*, vol. 80, no. 18, pp. 3346–3348, may 2002. [Online]. Available: https://doi.org/10.1063/1.1473868

[12] X. Zhang, H. Xie, M. Fujii, H. Ago, K. Takahashi, T. Ikuta, H. Abe, and T. Shimizu, "Thermal and electrical conductivity of a suspended platinum nanofilm," *Applied Physics Letters*, vol. 86, no. 17, p. 171912, apr 2005. [Online]. Available: https://doi.org/10.1063/1.1921350

[13] Q. G. Zhang, X. Zhang, B. Y. Cao, M. Fujii, K. Takahashi, and T. Ikuta, "Influence of grain boundary scattering on the electrical properties of platinum nanofilms," *Applied Physics Letters*, vol. 89, no. 11, p. 114102, sep 2006. [Online]. Available: https://doi.org/10.1063/1.2338885

[14] S. Ecoffey, J.-F. Morissette, N. Jedidi, M. Guilmain, C. Nauenheim, and D. Drouin, "Ultrathin titanium passive devices fabrication," in *2011 11th IEEE International Conference on Nanotechnology*. IEEE, aug 2011. [Online]. Available: https://doi.org/10.1109/nano.2011.6144494

[15] M. Day, M. Delfino, J. Fair, and W. Tsai, "Correlation of electrical resistivity and grain size in sputtered titanium films," *Thin Solid Films*, vol. 254, no. 1-2, pp. 285–290, jan 1995. [Online]. Available: https://doi.org/10.1016/0040-6090(94)06259-n

[16] A. Taylor, M. Cordill, L. Bowles, J. Schalko, and G. Dehm, "An elevated temperature study of a Ti adhesion layer on polyimide," *Thin Solid Films*, vol. 531, pp. 354–361, mar 2013. [Online]. Available: https://doi.org/10.1016/j.tsf.2013.01.016

[17] R. A. Meirom, D. H. Alsem, A. L. Romasco, T. Clark, R. G. Polcawich, J. S. Pulskamp, M. Dubey, R. O. Ritchie, and C. L. Muhlstein, "Fatigue-induced grain coarsening in nanocrystalline platinum films," *Acta Materialia*, vol. 59, no. 3, pp. 1141–1149, feb 2011. [Online]. Available: https://doi.org/10.1016/j.actamat.2010.10.047